AL-Bahir
Journal for Engineering and Pure Sciences
BJEPS

Manuscript 1119

Development and Evaluation of a Smart Vacuum-Assisted Suspension System for Transtibial Prostheses

Zahraa Kathem Ali

Wajdi Sadik Aboud

ORIGINAL STUDY

Development and Evaluation of a Smart Vacuum-assisted Suspension System for Transtibial Prostheses

Zahraa K. Ali [a,*], Wajdi S. Aboud [b]

[a] Prosthetics and Orthotics Engineering Department, University of Al-Nahrain, Baghdad, Iraq
[b] Artificial Intelligence Engineering Department, University of Al-Nahrain, Baghdad, Iraq

Abstract

A prosthetic socket is essential for achieving comfort, gait symmetry, and overall satisfaction for amputees. Effective suspension systems are crucial for securely attaching prostheses, thereby optimizing comfort, functional performance, and long-term limb health. This study aimed to develop and evaluate an intelligent vacuum-assisted suspension system for transtibial prostheses to improve socket fit, gait stability, and reduce residual limb movement. The system integrates force-sensitive resistors (FSRs) and an inertial measurement unit (MPU6050) with accelerometer and gyroscope sensors, continuously monitoring interface pressure and limb motion. Real-time data from these sensors dynamically adjusts vacuum pressure based on the user's gait pattern. Quantitative gait analysis conducted with the G-Walk system under non-vacuum and vacuum conditions identified biomechanical deficiencies without vacuum, including reduced gait quality, decreased stride length, and asymmetrical pelvic motion. When the vacuum system was activated, walking speed increased from 0.88 m/s to 1.04 m/s (~18 %), propulsion force improved from 5.5 N to 8.0 N, and the symmetry index rose from 74.7 % to 83.3 %, reflecting more efficient push-off, enhanced bilateral balance, and improved dynamic stability. These findings extend previous work, such as Gholizadeh et al. (2020) and Coburn et al. (2022), by not only confirming improvements in socket stability but also providing clear quantitative evidence of enhanced gait mechanics. Compared to Kent et al. (2024), who emphasized functional benefits of vacuum-assisted suspension, the present system demonstrates measurable biomechanical gains through dynamic, real-time vacuum regulation. Long-term functional measurements showed consistent improvements in stride uniformity and cadence, demonstrating the system's efficacy in enhancing limb-socket interaction, dynamic alignment, and overall gait efficiency. Because this study is based on a single case, the results are still preliminary and require confirmation through studies involving multiple participants.

Keywords: FSR, BK, Smart vacuum system, Suspension system

1. Introduction

A prosthetic socket is the essential element that links the residual limb to the lower limb prosthesis. This interface is crucial for comfort, gait symmetry, proprioception, and overall satisfaction among individuals with amputations. Consequently, selecting a suitable suspension system is a critical phase in prosthetic rehabilitation, ensuring the secure and efficient attachment of the prosthesis to the residual limb [1]. Proper suspension of prosthetic sockets onto the residual limb is key to optimizing comfort, functional performance, and long-term limb health in lower-limb amputees. Fluctuations in residual limb volume, daily and over prolonged periods, alter socket fit, leading to relative movement between the socket and residual limb, generally characterized as pistoning. This movement results in discomfort, skin breakdown, and reduced gait efficiency [2,3]. To address these problems, several studies have analyzed various vacuum-assisted suspension systems (VASS). Youngblood et al. (2020) provided a mechanical model simulating elevated vacuum suspension

Received 11 July 2025; revised 20 September 2025; accepted 21 September 2025.
Available online 29 December 2025

* Corresponding author at: Prosthetics and Orthotics Engineering Department, University of Al-Nahrain, Baghdad, Iraq.
E-mail addresses: msc.zahraakadim.po23@ced.nahrainuniv.edu.iq (Z.K. Ali), wajdisadik@gmail.com (W.S. Aboud).

https://doi.org/10.55810/2313-0083.1119

systems in prosthetic sockets, offering recommendations for optimal vacuum pressure management and tissue damage prevention [3]. Gholizadeh et al. (2020) mechanically evaluated the Unity elevated vacuum suspension system, confirming its effectiveness in improving socket stability and reducing limb movement within the socket during gait [4]. Youngblood (2019) examined both the physiological and mechanical effects of elevated vacuum systems, observing significant reductions in residual limb volume fluctuations and an improvement in socket-limb interaction [5]. Le et al. (2021) compared oxygen consumption and speed performance in an amputee runner using an elevated vacuum suspension system, demonstrating clear functional benefits in performance and comfort [6]. Major et al. (2015) compared the effectiveness of electric vacuum pumps for transfemoral prosthetic sockets, highlighting significant differences in vacuum creation efficiency and user convenience [7]. Komolafe et al. (2013) developed methods to characterize the mechanical and electrical performance of prosthetic vacuum pumps, providing benchmarks for performance evaluation [8]. Coburn et al. (2022) introduced an instrumented printed insert for continuous monitoring of distal limb motion and vacuum loss, addressing limitations in static vacuum suspension systems [9]. In addition, the protocol proposed by Klotz et al. (2023) demonstrated that repeated N-of-1 trial designs provide objective evidence of the effectiveness of vacuum-assisted suspension systems (Unity system) in terms of daily user comfort; however, it remained limited by focusing primarily on comfort as the main outcome measure [10]. Kent et al. (2024) explored how increased socket-residual limb coupling via vacuum-assisted suspension enhances prosthetic control, revealing improvements in sensory feedback and functional performance [11]. However, these studies underscore the need for an intelligent, integrated vacuum-assisted suspension system capable of dynamic, real-time adjustments tailored specifically to each user's biomechanical and physiological needs. This study presents how to combine and create a smart vacuum suspension system that has an electrically controlled vacuum pump, several FSRs placed in the socket in a strategic way, and an IMU to track the phases of walking. The system constantly adjusts the vacuum pressure to match the patient's movements. This improves the function of the prosthetic suspension, reduces the pistoning of the residual limb, and makes the user more comfortable and mobile. This new idea tries to fill in the gaps in current static vacuum suspension technology by providing an adaptive, user-sensitive solution that is uniquely designed to meet the biomechanical and physiological needs of each amputee.

2. Methods

The methodology adopted in this study consisted of two main phases: the fabrication of a transtibial prosthetic socket using standard clinical procedures, and the integration of a smart vacuum-assisted suspension system. The aim was to evaluate the effectiveness of the proposed system in improving socket fit and gait performance. Detailed procedures included patient selection, socket manufacturing, electronic system assembly, sensor calibration, and functional testing under real walking conditions.

2.1. Patient selection

A single participant (n = 1) with unilateral transtibial amputation was recruited from the Babylon Rehabilitation Center for Disabled Persons. The participant was a 23-year-old male with a traumatic left transtibial amputation sustained five years earlier. No chronic illnesses or dermatological conditions that might interfere with prosthesis use were reported. A conventional transtibial prosthesis without a vacuum-assisted suspension system had been previously used. For this study, a custom laminated composite transtibial socket with a total surface bearing (TSB) design was fabricated and fitted with a silicone liner matched to the residual limb. The participant met the following inclusion criteria: adult with unilateral transtibial amputation, at least six months post-amputation, absence of balance or gait problems, absence of open sores or infections on the residual limb, and correct socket fit. Table 1 presents the participants' characteristics, including age, gender, weight, height, cause, and time since amputation, socket and liner type, functional activity level, and the non-vacuum condition applied during testing.

The study protocol was reviewed and approved by the institutional ethics committee, and written informed consent was obtained before participation. All testing and monitoring procedures were conducted under the direct supervision of a licensed prosthetist and in accordance with ethical research standards.

2.2. Production of a below-the-knee prosthetic socket

Construction of a below-the-knee prosthetic socket involves accurate steps in measurement,

Table 1. Presents the participants' characteristics.

Parameter	Description
Age/Sex/Weight	23-year-old male, approximately XX kg
Cause & time since amputation	Traumatic left transtibial amputation, 5 years prior
Socket type	Custom transtibial socket, laminated composite materials, total surface bearing design
Liner type	Silicone liner (Ossur, size-matched to residual limb)
Baseline activity level	K4 functional level high mobility, independence, daily activities
Non-vacuum condition	Implemented by deactivating the miniature vacuum pump while maintaining the same socket liner setup (no auxiliary pin-lock used)

casting, and assembly for proper fitting and function. The process begins with Measurement and Marking, measuring the length of the sound limb and residual limb, and selecting a proper silicone liner according to the size and shape of the residual limb. Important areas like pressure tolerance and intolerable areas are identified on the limb to guarantee a functional and comfortable fit. The Negative Cast Preparation is then conducted by soaking a plaster of Paris roll in water, and it is wrapped around the limb, beginning from above the knee and proceeding down to the stump's end. Pressure is applied over the marked areas of tolerance, and upon hardening of the plaster, the cast is gently removed. In the Positive Cast Preparation, the negative mold is extended with additional plaster to form a positive cast. Gypsum and water are mixed and poured into the negative mold, left to harden, and become the positive mold of the residual limb. After that, the Rectification and Adding stage shapes the load-bearing areas and adds gypsum to the bony prominences. The cast is sculpted and shaped to achieve the desired final shape before moving to the lamination phase. During Lamination and Hard Modular Socket, the cast is put onto a vacuum equipment, and layers of Perlon and carbon fiber are applied over it. Lamina resin is infused into the layers, and the vacuum guarantees that air is removed between them. The resin hardens, and a strong and durable socket is formed. Lastly, the Assembly and Alignment stage entails attaching the shank to the socket through an adapter, then joining the foot to the shank. The alignment procedure is done in three phases: baseline, static (pre-use), and dynamic (post-use), to guarantee function, stability, and comfort for the user as illustrated in Fig. 1, the complete fabrication process includes key stages such as negative and positive casting, mold rectification, lamination, and final assembly of the transtibial socket.

2.3. Integration of a smart vacuum-assisted suspension system

As illustrated in Fig. 2. The developed transtibial prosthetic system integrates a vacuum-assisted suspension mechanism with embedded sensors and a microcontroller-based control unit. The system framework was structured to enhance socket limb coupling, minimize pistoning, and enable real-time monitoring through a modular arrangement of hardware and software components. The framework is divided into hardware integration, software and control logic, operational mechanism, prosthetic assembly, and evaluation of system limitations.

2.3.1. Hardware framework

2.3.1.1. Vacuum module. The vacuum generation unit consisted of a miniature brushless DC centrifugal pump (Model 36003, Fine Watt) with a measured weight of ~64 g. The pump operated at a rated voltage of 21.6 VDC with a maximum rotational speed of 50,000 rpm and a power consumption of 150 W. It was capable of producing suction pressures of up to 16 kPa at high speed and 9 kPa at low speed, with corresponding airflow rates of 20.5 dm^3/s and 15 dm^3/s. The pump was externally mounted on the lateral thigh to minimize socket loading and avoid interference with gait, while a flexible silicone hose connected the inlet to the socket chamber. As presented in Fig. (2-b) one-way valve was integrated to preserve vacuum during pump deactivation, and ventilation slots were incorporated in the 3D-printed housing to prevent overheating.

For clarity, the complete technical specifications of the pump are summarized in Table 2, which provides a detailed overview of its operating characteristics, including current draw, bearing type, control method, and efficiency.

2.3.1.1.1. Bench testing and calibration of the vacuum pump. To ensure clinical usability, the miniature vacuum pump was subjected to bench calibration tests using a digital pressure sensor placed inside the socket chamber for continuous monitoring. Upon activation, the pump reduced the chamber pressure to −4 kPa within ~12 s, a level intentionally selected as clinically safe and below the manufacturer's maximum rating (−16 kPa) to ensure user comfort and tissue safety.

Vacuum stability under load and leak was evaluated by maintaining the system in a sealed

Fig. 1. Fabrication process of a transtibial (below-the-knee) prosthetic socket.

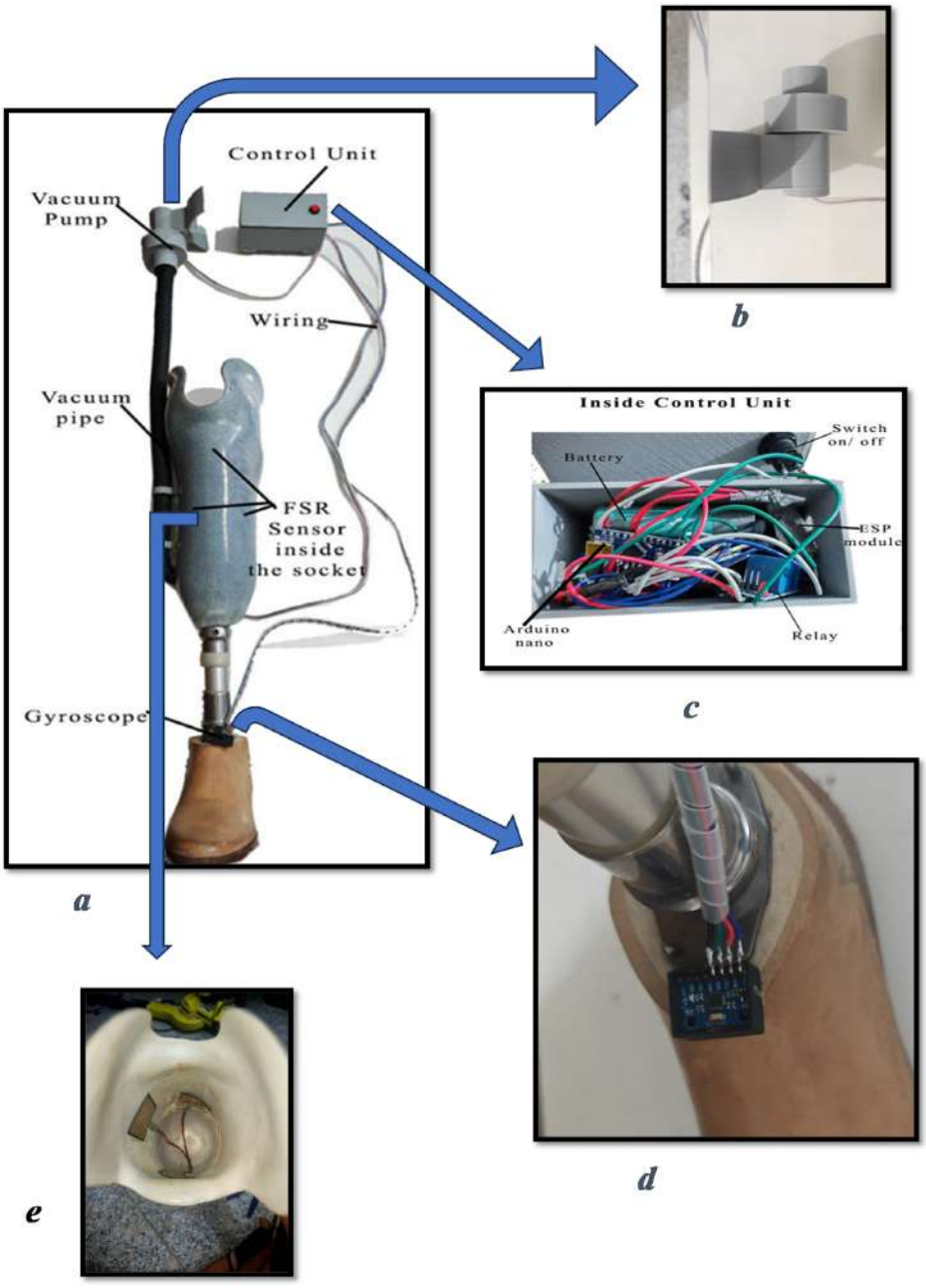

Fig. 2. Components of the smart vacuum-assisted suspension system. (a) Complete transtibial prosthesis fitted with the smart vacuum-assisted suspension. (b) Vacuum Module. (c) Inside view of the control unit, including Arduino Nano, ESP module, relay, battery, and switch. (d) The MPU6050 accelerometer gyroscope module. (e) FSR sensor placed inside the socket.

condition for 1 min, during which the pressure plateau remained stable with minimal fluctuations. A controlled leak was then introduced by partially venting the chamber, resulting in a gradual pressure rise of ~0.1 kPa/min. Once reactivated, the pump restored the vacuum level to −4 kPa within a few seconds, confirming its ability to recover after leakage. Battery runtime was assessed in two modes:

Continuous mode: ~0.26 h (15 min).

Intermittent (gait-triggered) mode: ~0.5 0.7 h.

Lifting performance was also tested to illustrate the effect of hose length on suction efficiency. As shown in Fig. 3, the lifted weight increased proportionally with suction cup diameter in the baseline configuration. However, the inclusion of a 50-cm hose significantly reduced lifting capacity across all diameters. At a reference suction diameter of

Table 2. Technical specifications of the vacuum pump.

Specification	Value
Pump Type	Brushless DC, centrifugal
Model Number	36003
Rated Voltage	21.6 VDC
Power Consumption	150 W
Maximum Rotational Speed	50,000 RPM
Suction Pressure (High Speed)	16 kPa
Suction Pressure (Low Speed)	9 kPa
Airflow Rate (High Speed)	20.5 dm^3/s
Airflow Rate (Low Speed)	15 dm^3/s
Current Draw (High Speed)	6.94 A
Current Draw (Low Speed)	3.7 A
Bearing Type	Ball Bearing
Weight (Measured)	~64 g
Control Method	External electronic controller

2.5 cm, the original configuration lifted ~200 g, whereas the hose-extended configuration lifted only ~140 g, highlighting the pressure losses introduced by tubing.

Collectively, these findings demonstrate that the pump reliably achieves and maintains the clinically safe vacuum (−4 kPa), recovers rapidly under leakage, and exhibits performance reductions when extended hose lengths are used, validating its suitability for prosthetic integration.

2.3.1.2. Sensing units

1. Force Sensing Resistors (FSRs)

The system incorporates three FSR-406 sensors embedded inside the prosthetic socket at the medial, lateral, and posterior regions as shown in Fig. (2-e). To ensure clinical accuracy, calibration was performed with the sensors secured by medical-grade elastic tape, replicating the actual in-socket configuration. Reference loads ranging from 0 N to 90 N were sequentially applied using calibrated weights, and sensor outputs were simultaneously compared with a Tekscan F-Socket benchmark. The outcomes, presented in Fig. (4) and summarized in Table (3), revealed near-linear responses ($R^2 > 0.96$) with a small error margin of ±2.04 N as demonstrated in Table 4. This confirmed that the proposed calibration strategy provided reliable in-socket force measurements despite the damping effect of the liner and fixation tape.

2. The MPU6050 accelerometer gyroscope module

The MPU6050 accelerometer gyroscope module was mounted at the ankle foot junction, the

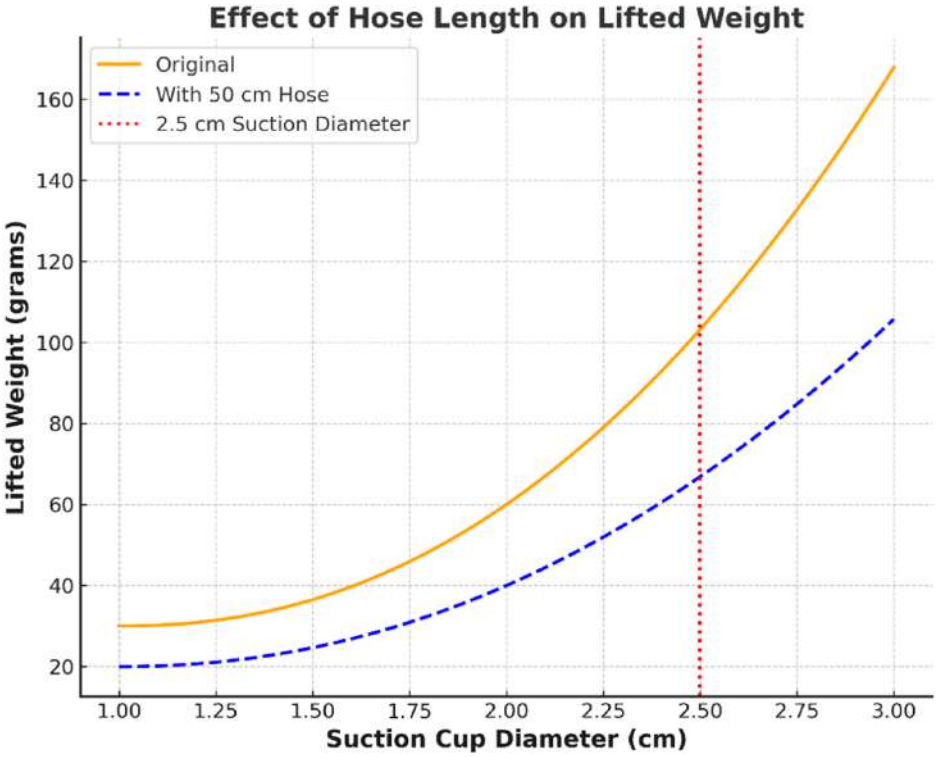

Fig. 3. Calibration test of the vacuum pump performance showing the effect of hose length on the lifted weight.

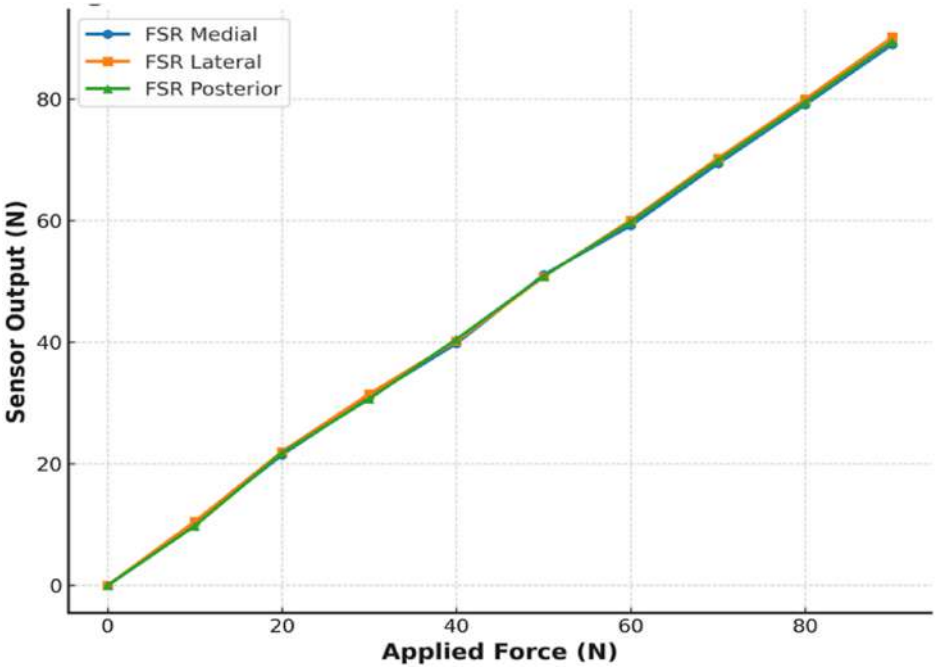

Fig. 4. Calibration curves of the three FSR-406 sensors (medial, lateral, and posterior).

location most sensitive to angular changes during gait Fig. (2-d). Calibration was conducted in two distinct stages. In the static calibration, the prosthetic limb was held stationary to establish zero-offset values and minimize sensor drift. In the dynamic calibration, controlled forward backward tilt cycles were applied through a mechanical hinge, with outputs validated against a digital inclinometer. Fig. (5) illustrates the calibration setup and sensor orientation, highlighting the MPU6050 placement for optimal sensitivity to pitch angles. Based on these trials, angular thresholds were defined as ±10° for heel strike and toe-off, while near-zero values (±5°) were representative of mid-stance. This dual calibration strategy ensured that both pressure and angular measurements were physiologically meaningful and reliable, thereby triggering the vacuum pump only during true gait transition phases.

Table 3. Summarizes the calibration data of FSR-406 sensors under applied reference loads (0 90 N), including raw readings, mean values, and standard deviations.

Reference Force (N)	FSR Front (N)	FSR Side 1 (N)	FSR Side 2 (N)	Mean (N)	SD (±N)
0.0	0.0	0.0	0.0	0.0	0.0
10.0	10.2	10.5	9.8	10.17	0.35
20.0	21.5	22.0	21.8	21.77	0.25
30.0	31.0	31.5	30.7	31.07	0.4
40.0	39.8	40.2	40.5	40.17	0.35
50.0	51.1	50.8	50.9	50.93	0.15
60.0	59.2	60.1	59.8	59.7	0.46
70.0	69.4	70.3	69.9	69.87	0.45
80.0	79.1	80.0	79.5	79.53	0.45
90.0	89.0	90.2	89.5	89.57	0.6

2.3.1.3. Power configuration. The 7.4 V dual-cell Li-ion battery powered the pump, sensors, and microcontroller. Under continuous operation, the system provided >8 h of active use. An LED indicator displayed charge levels, and the BMS maintained safe charging and discharging.

The vacuum pump alone weighed approximately 67 g, and together with the electronic control unit, the added load remained within acceptable limits for transtibial prostheses. Strategic placement ensured that weight did not interfere with ambulation: the pump was externally fixed to the lateral thigh with an elastic strap, while the control unit was housed in a lightweight 3D-printed PLA box as shown in Fig. (2-c) mounted at the waist. This configuration distributed mass away from the

Table 4. Presents the linear regression parameters, demonstrating high linearity ($R^2 > 0.96$) and confirming the reliability of the in-socket calibration procedure.

Sensor	Slope	Intercept	R^2
FSR Front (N)	0.981	0.8836	0.9994
FSR Side 1 (N)	0.9916	0.9364	0.9996
FSR Side 2 (N)	0.9888	0.7418	0.9995

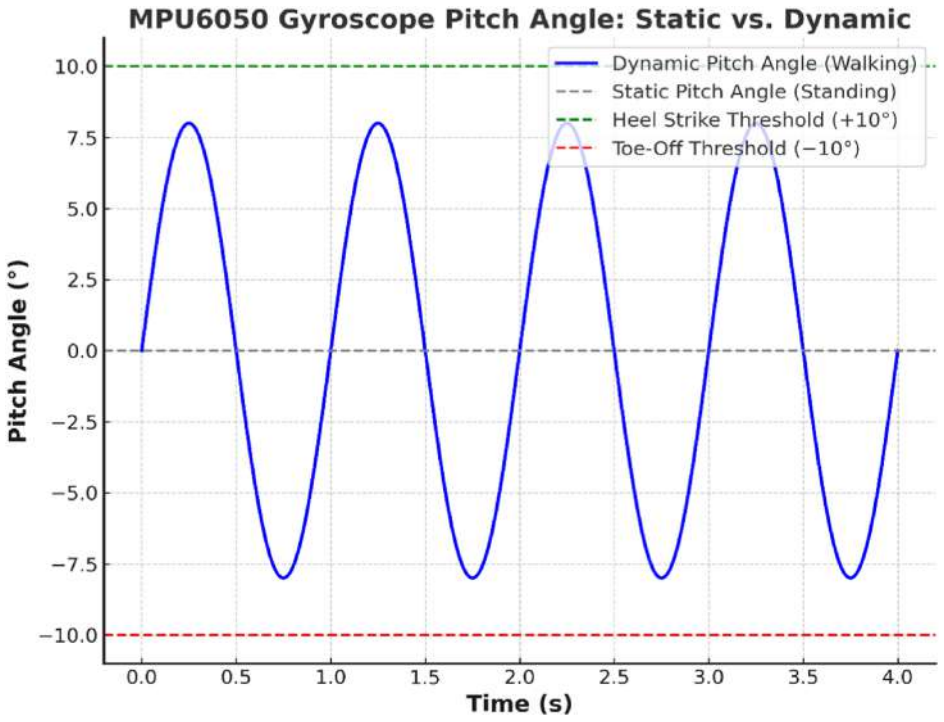

Fig. 5. Calibration results of the MPU6050 accelerometer gyroscope module sensor under static (standing) and dynamic (walking) conditions.

socket, preserving suspension stability and user comfort.

2.3.1.4. Wiring and vacuum pump. The wiring network provided the essential electrical connections between the sensors, control unit, and vacuum pump. Flexible insulated wires were routed externally along the socket wall to minimize bulk and ensure free limb movement, while maintaining stable signal transmission and power delivery.

The miniature vacuum pump (outer diameter 25 mm) was responsible for generating negative pressure within the socket through a dedicated vacuum pipe. By creating a controlled suction of up to −4 kPa, the pump enhanced socket limb coupling and reduced pistoning. A one-way valve preserved the vacuum when the pump was deactivated, while the control unit regulated its activation based on sensor input as illustrated in Fig. (2-a). This configuration ensured stable suspension, reduced energy consumption, and maintained clinical usability during gait.

2.3.1.5. Control circuitry. The control circuitry of the smart vacuum-assisted prosthetic system was implemented **as presented in** Fig. (6)**.** At the core of the design, an Arduino Nano microcontroller served as the primary processing unit, acquiring and interpreting biomechanical signals from multiple sensors and coordinating the actuation of the vacuum pump. Three Force Sensing Resistors (FSRs) were embedded inside the prosthetic socket at the medial, lateral, and posterior regions of the residual limb interface. These sensors were

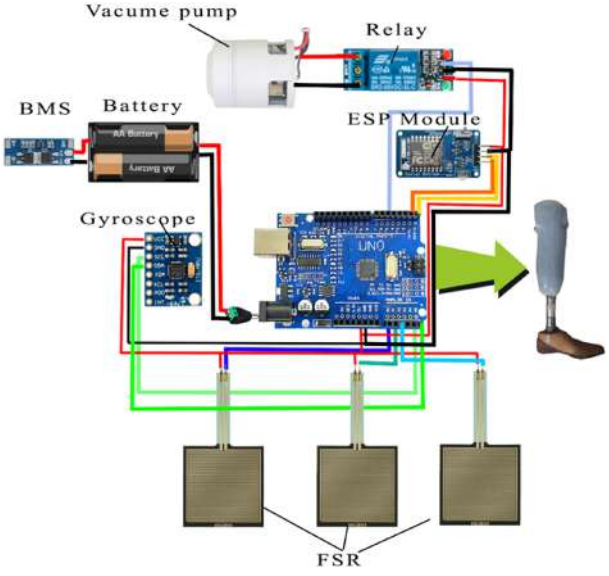

Fig. 6. Control circuitry of the smart vacuum-assisted suspension system.

connected to the analog input pins (A0 A2) of the Arduino Nano, enabling real-time detection of pressure variations during ambulation. In parallel, an MPU6050 gyroscope accelerometer module was integrated via the I^2C interface (A4 SDA and A5 SCL), providing continuous orientation data such as pitch angle and angular acceleration, which are essential for gait phase recognition.

Vacuum regulation was achieved through a relay module connected to digital pin D5, which electrically isolated the microcontroller from the high-current pump, ensuring safe switching. Pump activation was permitted only under two simultaneous conditions:

1. Pressure detected by the FSRs dropped below the defined contact threshold.
2. Angular tilt exceeded ±10°, corresponding to heel strike or toe-off phases.

Wireless connectivity was established using an ESP32/ESP8266 module, interfaced via UART (RX/TX), to transmit real-time sensor data and system status to an external monitoring dashboard. This allowed clinicians to visualize pressure and angular profiles, remotely control the system, and log gait sessions.

The circuit was powered by a 7.4 V lithium-ion battery pack managed by a Battery Management System (BMS) to protect against overcharging, over-discharging, and short circuits. A buck converter stepped the voltage down to 5 V to supply the Arduino Nano, sensors, relay, and wireless module. All wiring followed color-coded and shielded paths with a unified ground reference to minimize electrical noise and electromagnetic interference.

The hardware modules were organized in a modular arrangement: the vacuum pump was externally mounted on the lateral thigh, while the control electronics were enclosed in a lightweight 3D-printed PLA housing secured to a waist belt. This separation reduced socket load, improved user comfort, and facilitated system maintenance. Flexible conduits were used to route sensor wiring securely, preserving both user mobility and device durability.

2.3.2. Software framework and embedded data acquisition module

The software framework combined a closed-loop control algorithm on the Arduino Nano with a web server hosted by the ESP8266 module. This integration enabled automatic regulation of vacuum pressure and real-time remote monitoring. The Arduino Nano continuously processed input from three in-socket FSRs and an ankle-mounted MPU6050 IMU at a sampling frequency of 100 Hz. Pump activation was conditioned upon two triggers: (1) FSR values dropping below a predefined threshold, and (2) IMU pitch angle exceeding ±10°, corresponding to heel strike or toe-off. Once the negative pressure reached −4 kPa, the pump automatically deactivated, and a one-way valve preserved the vacuum. Safety features included a programmed suction cap of −4 kPa and a calibrated exhaust vent to prevent over-pressurization.

The ESP8266 web server provided a user interface accessible from a computer without requiring additional software. As shown in Fig. 7, the dashboard displayed real-time FSR pressure curves and IMU pitch angles, enabling clinicians to track socket loading patterns across gait phases. It also included a manual ON/OFF control for the pump and supported basic session logging with optional alert functions in case of abnormal readings.

To clearly illustrate this control logic, a flowchart was developed (Fig. 8), showing the sequential process from system initialization and sensor data acquisition to conditional pump activation and data transmission to the web server. This integrated framework ensured efficient pump actuation only during true gait transitions, minimized energy consumption, and allowed clinicians to supervise performance remotely, thereby enhancing both suspension stability and usability.

2.4. Operational mechanism

The smart vacuum-assisted socket operates through a closed-loop control framework integrating pressure and angular feedback. Three FSR sensors embedded within the socket monitor real-time contact pressure between the residual limb and the socket wall. Simultaneously, an MPU6050 gyroscope accelerometer mounted at the ankle foot junction detects sagittal plane tilt, with angular thresholds defined as ±10° for gait transitions and ±5° for mid-stance.

The Arduino Nano continuously processes these sensor inputs at 100 Hz. Pump activation is conditioned upon two simultaneous triggers: (1) FSR values dropping below the contact threshold, and (2) IMU tilt exceeding ±10°, corresponding to heel strike or toe-off. This dual-condition logic ensures suction is delivered only during genuine gait transitions, reducing false activations. Once negative pressure reaches −4 kPa, the pump deactivates

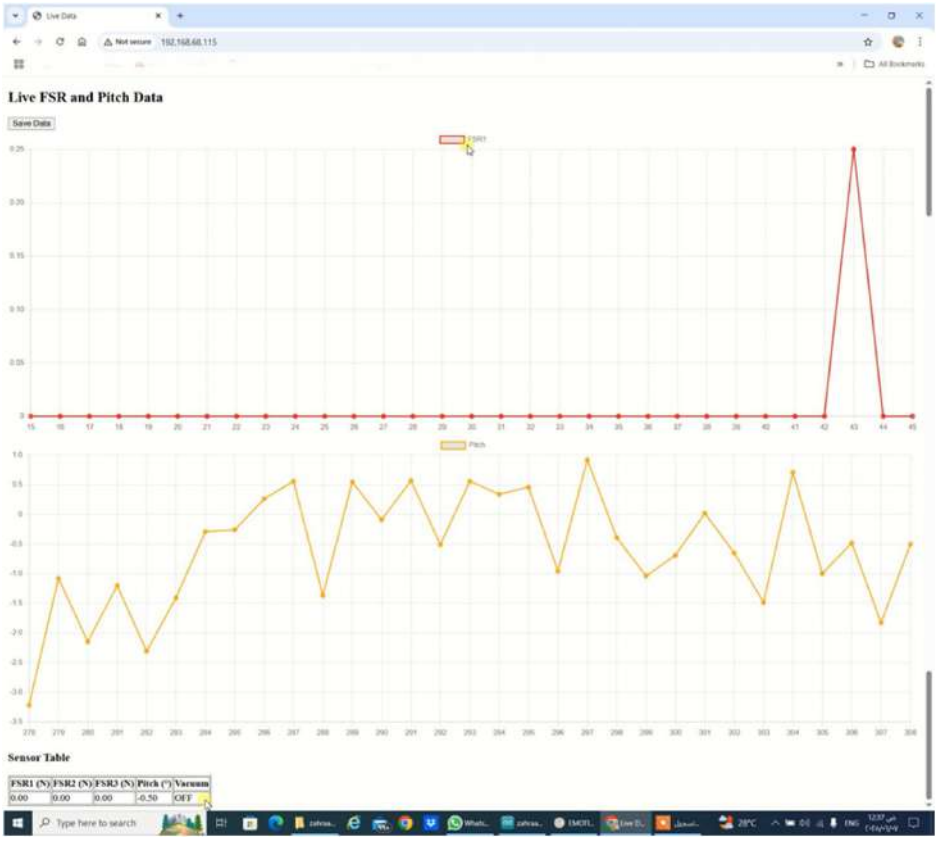

Fig. 7. Web-based interface of the ESP8266 module showing live FSR pressure data and gyroscope pitch angle, with vacuum status, manual ON/OFF control, and session logging.

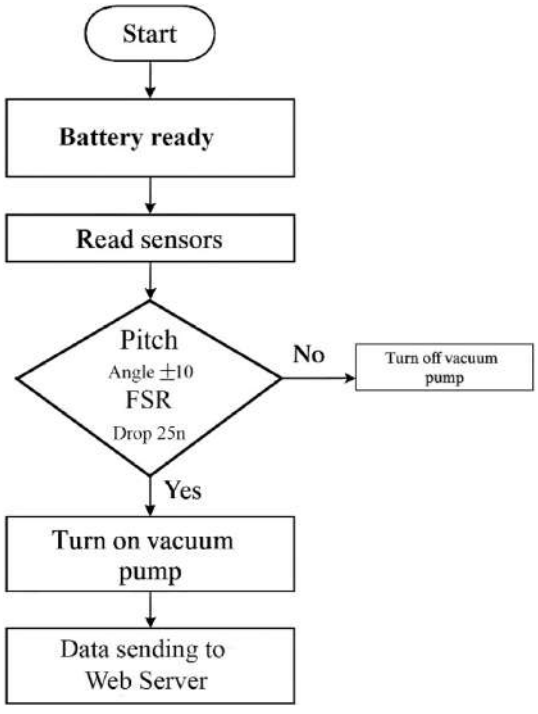

Fig. 8. Flowchart of the control logic implemented on the Arduino Nano, illustrating sensor input processing, threshold evaluation, pump activation/deactivation, and data transmission.

automatically, while a one-way valve preserves sub-atmospheric pressure passively. This cycling pattern minimizes energy consumption, prolongs pump lifespan, and prevents unnecessary noise or vibration.

All sensor data is transmitted in real time to a web interface hosted by the ESP8266 module. The dashboard provides live visualization of FSR pressure curves and gyroscopic pitch angles, along with manual ON/OFF control and basic session logging.

The vacuum pump is externally mounted on the lateral thigh via an elastic strap, while the control unit is housed in a lightweight PLA 3D-printed box secured at the waist. This modular arrangement reduces socket load, maintains user comfort, and prevents interference with gait mechanics.

3. Results

To evaluate the integration and functional performance of the developed smart vacuum-assisted suspension system, an experimental protocol was conducted under controlled laboratory conditions at the Department of Prosthetics and Orthotics,

Al-Nahrain University. The primary objective was to assess potential improvements in socket fit, gait dynamics, and user stability. A transtibial amputee participant was equipped with the G-Walk inertial measurement system, which was securely positioned at the L5 vertebral level using an adjustable elastic belt to ensure accurate motion tracking during walking trials (Fig. 9). The G-Walk is specifically designed for rapid and precise assessment of gait, running, and jumping, and comprises an inertial sensor (G-SENSOR), standardized movement analysis protocols, and the dedicated G-Studio software. In this study, it was employed to collect objective biomechanical parameters under two distinct conditions: with and without vacuum assistance. The recorded variables included walking speed, cadence, stance phase duration, propulsion force, and symmetry index.

Fig. 9. Experimental setup showing the transtibial amputee participant fitted with the smart vacuum-assisted suspension system.

3.1. Gait analysis without vacuum assistance

The initial walking assessment, conducted without activation of the vacuum system, demonstrated several biomechanical limitations. The walking speed was reduced to 0.88 ± 0.07 m/s, accompanied by a low cadence of 94.08 ± 8.31 steps/min, both below normal reference values. The prosthetic (left) limb exhibited a relatively shortened step length (53.25 %) compared with the contralateral side (46.75 %), indicating gait asymmetry. The stance phase of the sound limb was markedly prolonged (66.92 %) relative to the prosthetic side (55.13 %), reflecting reduced efficiency and compensatory loading.

The propulsion force generated by the prosthetic limb was limited to 5.5 N, while the contralateral limb reached 7.2 N. This imbalance was consistent with the low symmetry index (74.7 %), highlighting impaired inter-limb coordination. Furthermore, deviations in spatio-temporal parameters, including increased gait cycle duration (1.30 s) and reduced stride length (1.10 1.17 m), confirmed inefficiencies in forward progression. Collectively, these findings illustrate restricted dynamic stability, diminished propulsion, and poor postural control prior to vacuum assistance as shown in Figs. (10) and (11).

3.2. Gait analysis with vacuum assistance

Following activation of the vacuum-assisted suspension system, marked improvements in gait performance were observed. Walking speed increased to 1.04 ± 0.05 m/s, with a cadence of 94.23 ± 4.69 steps/min, approaching normal values. Both stride length (1.30 m left, 1.28 m right) and step length symmetry improved, with left and right steps recorded at 49.72 % and 50.28 %, respectively, indicating more balanced forward progression.

The stance and swing phases demonstrated a closer approximation to physiological values, with the prosthetic (left) limb showing a stance phase of 54.99 % and swing of 45.01 %, while the sound (right) limb displayed a stance of 59.51 % and swing of 40.49 %. These distributions reflect enhanced temporal symmetry and reduced compensatory loading.

Propulsion forces significantly improved on both sides, reaching 8.0 N for the prosthetic limb and 8.4 N for the sound limb, in contrast to the reduced propulsion measured before vacuum activation. Moreover, the symmetry index increased to 83.3 %, indicating enhanced inter-limb coordination as shown in Figs. (12 and 13).

Spatio-Temporal parameters	Value (Mean ± Std Dev)	Normal Value (Mean ± Std Dev)
Analysis duration (s)	17.7	
Cadence (steps/min)	94.08 ± 8.31	118.80 ± 7.80
Speed (m/s)	0.88 ± 0.07	1.23 ± 0.11

Spatio-Temporal parameters	Left Value (Mean ± Std Dev)	Right Value (Mean ± Std Dev)	Normal Value (Mean ± Std Dev)
Gait cycle duration (s)	1.29 ± 0.05	1.30 ± 0.01	1.12 ± 0.15
Stride length (m)	1.17 ± 0.05	1.10 ± 0.04	1.23 ± 0.07
% Stride length (% height)	66.58 ± 2.93	63.13 ± 2.56	84.70 ± 6.10
Step length (% str length)	53.25 ± 4.26	46.75 ± 2.94	50.00 ± 0.70
Elaborated steps	3	3	

Fig. 10. G-Walk spatio-temporal gait parameters before vacuum activation, showing improved walking efficiency and balanced stance swing distribution.

Collectively, these post-vacuum results confirm that the smart suspension system improved dynamic stability, propulsion capacity, and gait symmetry, thereby reducing biomechanical deficiencies observed during the initial (non-vacuum) condition.

3.3. Six-Minute Walk Test (6MWT)

The 6MWT showed a significant improvement in endurance and gait continuity. Without a vacuum, the patient walked 292.9 m; with vacuum activation, this distance increased to 324.5 m. This indicates improved comfort and reduced fatigue during extended walking. Additional gait parameters including walking speed, stance phase, propulsion force, and symmetry index also showed notable improvements with vacuum assistance, as detailed in Table 5. Importantly, the vacuum pump was not continuously active during the trial; instead, it was automatically triggered several times based on the predefined activation thresholds, ensuring stable suspension while minimizing unnecessary energy consumption.

4. Discussion

The results demonstrated clear improvements in gait mechanics when the smart vacuum-assisted suspension system was activated. Under vacuum conditions, the participant achieved a higher walking speed (0.88 m/s increased to 1.04 m/s) and greater propulsion force (5.5 N increased to 8.0 N on the prosthetic side), reflecting more efficient push-off and energy transfer during ambulation.

Walking speed improved by approximately 18 %, while stance phase duration decreased from 66.92 % to 59.51 %, indicating enhanced dynamic movement and reduced compensatory loading. The symmetry index also rose from 74.7 % to 83.3 %, highlighting improved bilateral gait balance. Furthermore, endurance improved, as evidenced by the Six-Minute Walk Test, in which the covered distance increased from 292.9 m without vacuum to

Spatio-Temporal parameters	Value (Mean ± Std Dev)	Normal Value (Mean ± Std Dev)
Analysis duration (s)	17.7	
Cadence (steps/min)	94.23 ± 4.69	118.80 ± 7.80
Speed (m/s)	1.04 ± 0.05	1.23 ± 0.11

Spatio-Temporal parameters	Left Value (Mean ± Std Dev)	Right Value (Mean ± Std Dev)	Normal Value (Mean ± Std Dev)
Gait cycle duration (s)	1.26 ± 0.03	1.24 ± 0.01	1.12 ± 0.15
Stride length (m)	1.30 ± 0.05	1.28 ± 0.01	1.23 ± 0.07
% Stride length (% height)	74.35 ± 2.95	73.22 ± 0.29	84.70 ± 6.10
Step length (% str length)	49.72 ± 2.27	50.28 ± 1.56	50.00 ± 0.70
Elaborated steps	4	4	

Fig. 11. G-Walk spatio-temporal gait parameters after vacuum activation, showing improved walking efficiency and balanced stance -swing distribution.

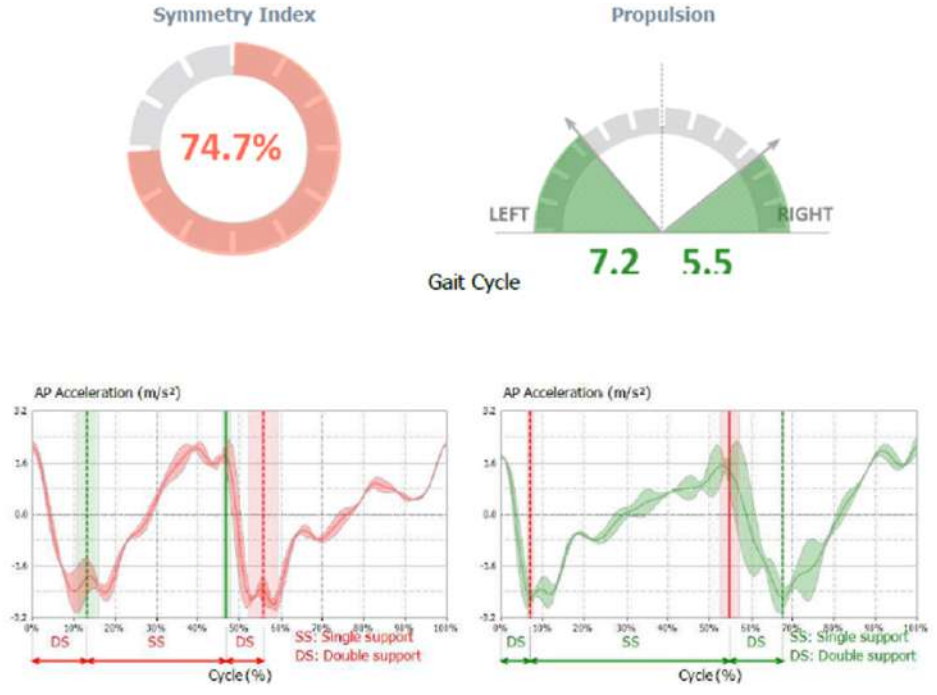

Fig. 12. G-Walk symmetry index, propulsion, and AP acceleration curves before vacuum activation.

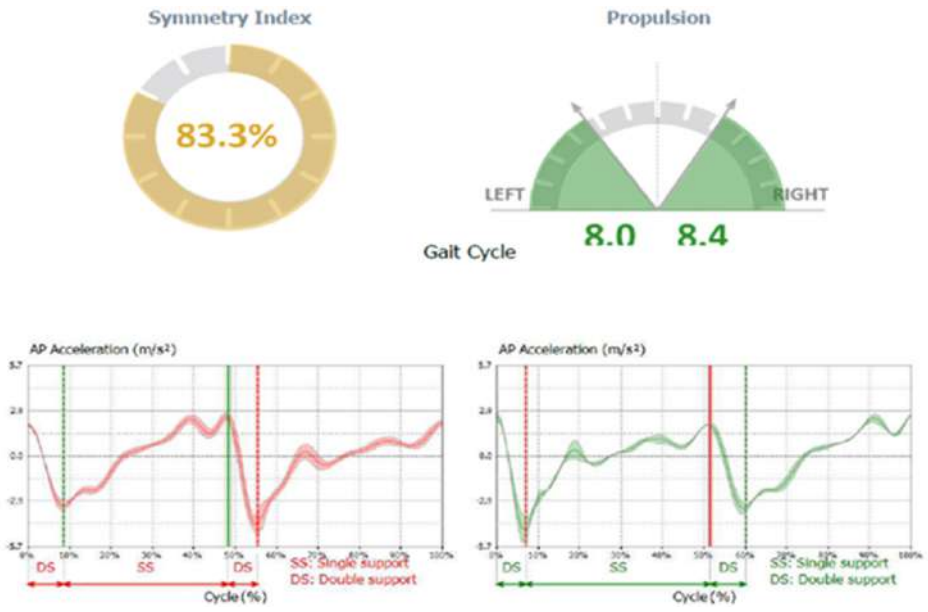

Fig. 13. G-Walk symmetry index, propulsion, and AP acceleration curves after vacuum activation.

324.5 m with vacuum activation. Collectively, these findings suggest that the smart vacuum-assisted suspension enhanced socket limb coupling, reduced pistoning, and promoted smoother forward progression with greater stability and confidence in weight-bearing.

Despite these promising outcomes, several limitations must be acknowledged. The study was conducted as a single-subject case study (N = 1), which restricts the generalizability of the findings and precludes the use of statistical analysis or inferential conclusions. Moreover, the participant was a young, active individual classified at the K4 functional level, which contrasts with the broader amputee population, typically older and presenting with comorbidities.

Another limitation concerned the vacuum pump: although the selected unit successfully generated the required negative pressure, it produced a noticeable noise level during operation, which could potentially affect user comfort in daily life. In addition, the external positioning of the control unit and the extensive wiring between components mainly influenced the system's aesthetic appearance, reducing visual appeal without significantly compromising portability or functionality.

Collectively, these limitations highlight the need for further studies involving larger and more diverse participant groups, along with technical optimization of pump design, material selection, and system integration to enhance both clinical applicability and daily usability. While the present findings suggest potential benefits in gait stability and comfort, confirmation in larger, randomized controlled trials remains essential.

Table 5. Gait parameters recorded under non-vacuum and vacuum-assisted conditions.

Parameter	Without Vacuum	With Vacuum
Walking Speed (m/s)	0.88	1.05
Stance Phase (%)	66.92	61.91
Propulsion Force (N)	5.5	7.2
Symmetry Index (%)	74.7	92.9
6MWT Distance (m)	292.9	324.5

5. Conclusion

The preliminary findings of this study demonstrate that the smart vacuum-assisted suspension system improved functional and biomechanical performance in a transtibial prosthesis user. With vacuum activation, walking became more efficient, propulsion increased, gait symmetry was enhanced, and endurance improved, indicating better socket limb coupling and reduced pistoning during ambulation. These outcomes highlight the potential of the system to promote smoother forward progression and greater stability in daily use.

However, several limitations must be considered. The study was conducted on a single participant, which restricts the generalizability of the results and prevents statistical validation. The participant's relatively young age and high functional level may also not reflect the broader amputee population, who are often older and present with comorbidities.

In addition, the external positioning of the control unit and the presence of multiple connecting wires primarily affected the aesthetic appearance of the system, rather than its functionality or portability.

Future research should therefore involve larger and more diverse participant groups, including different age ranges, causes of amputation, and activity levels, to confirm the clinical benefits of the system and enhance its reliability. Further refinement of the pump design, socket integration, and electronic components is also recommended to improve usability, aesthetics, and acceptance in daily practice.

Source of Funding

The authors declare that no funds, grants, or other support were received during the preparation of this manuscript.

Conflict of Interest

The authors declare that the research was conducted in the absence of any commercial or financial relationships that could be construed as a potential conflict of interest.

Ethical Approval

This study received approval from the Ethics Committee of the Department of Prosthetics and Orthotics Engineering at Al-Nahrain University's College of Engineering. The research was conducted in strict adherence to the ethical guidelines and standards set forth by the committee. Written informed consent was obtained from the participant prior to their inclusion in the study.

Data Availability

The datasets generated for this study contain sensitive information and are not publicly available due to participant privacy. However, the data can be made available from the corresponding author upon reasonable request.

Author Contributions

Zahraa Kathem Ali: Conceptualization; Methodology; Writing Original Draft Preparation; Visualization; Data Curation.

Wajdi Sadik Aboud: Supervision; Validation; Writing Review & Editing; Resources; Project Administration.

Both authors have read and agreed to the published version of the manuscript.

Acknowledgments

The authors express their sincere gratitude to the Nahrain University Library for providing access to essential academic resources. Special thanks are also extended to the laboratories of the Department of Prosthetics and Orthotics Engineering for their generous assistance and for providing the necessary facilities for this study. The authors are also grateful to the prosthetic centers, particularly Baghdad Prosthetic Center for their valuable assistance in the data collection process and for their cooperation during the study. Their support was crucial for the successful completion of this research.

References

[1] Thibault G, Gholizadeh H, Sinitski E, Baddour N, Lemaire ED. Effects of the Unity vacuum suspension system on transtibial gait for simulated non-level surfaces. PLoS One 2018;13(6):e0199181. https://doi.org/10.1371/journal.pone.0199181.

[2] Klute GK, Berge JS, Biggs W, Pongnumkul S, Popovic Z, Curless B. Vacuum-assisted socket suspension compared with pin suspension for lower extremity amputees: effect on fit, activity, and limb volume. Arch Phys Med Rehabil 2011; 92(10):1570 5. https://doi.org/10.1016/j.apmr.2011.05.019.

[3] Youngblood RT, Hafner BJ, Czerniecki JM, Brzostowski JT, Allyn KJ, Sanders JE. Modeling the mechanics of elevated vacuum systems in prosthetic sockets. Med Eng Phys 2020; 84:75 83. https://doi.org/10.1016/j.medengphy.2020.07.019.

[4] Gholizadeh H, Lemaire ED, Salekrostam R. Mechanical evaluation of the Unity elevated vacuum suspension system. Can Prosthet Orthot J 2020;2(2):32941. https://doi.org/10.33137/cpoj.v2i2.32941.

[5] Youngblood RT. Physiological and mechanical effects of prosthetic elevated vacuum systems in people with transtibial amputation (Doctoral dissertation). 2019.

[6] Le H, Guerra G, Sasaki K, Phongphibool S, Smith JD, Wongpanya J, et al. Oxygen consumption and speed performance of a runner with amputation wearing an elevated vacuum running prosthesis. JPO J Prosthetics Orthot 2021; 33(1):73 9. https://doi.org/10.1097/JPO.000000000000031. .

[7] Major MJ, Caldwell R, Fatone S. Comparative effectiveness of electric vacuum pumps for creating suspension in transfemoral sockets. JPO J Prosthetics Orthot 2015;27(4): 149 53.

[8] Komolafe O, Wood S, Caldwell R, Hansen A, Fatone S. Methods for characterization of mechanical and electrical prosthetic vacuum pumps. J Rehabil Res Dev 2013;50(8). https://doi.org/10.1097/JPO.0000000000000073. .

[9] Coburn KA, DeGrasse NS, Mertens JC, Allyn KJ, McCarthy NK, Ballesteros D, et al. An instrumented printed insert for continuous monitoring of distal limb motion in suction and elevated vacuum sockets. Prosthesis 2022;4(4): 710 29. https://doi.org/10.3390/prosthesis4040056.

[10] Klotz R, Emile G, Daviet JC, De Seze M, Godet J, Urbinelli R, et al. Daily socket comfort in transtibial amputee with a vacuum-assisted suspension system: study protocol of a randomized, multicenter, double-blind multiple N-of-1 trial. BMC Sports Sci Med Rehabil 2023;15(1):85.

[11] Kent JA, Carnahan KJ, Major MJ. Exploring the effects of increased socket-residual limb coupling integrity via vacuum-assisted suspension on prosthetic control: a preliminary study in transtibial prosthesis users. Disabil Rehabil 2025;47(9):2450 8. https://doi.org/10.1080/09638288.2024.2395454. .